Serum Molecular Biomarkers in Neuromyelitis Optical and Multiple Sclerosis

Cong-Cong Fu
Guangzhou Medical University Second Affiliated Hospital
Cong Gao
Guangzhou Medical University Second Affiliated Hospital
Hui-Hua Zhang
Shenzhen University
Ying-Qing Mao
RayBiotech Life, Inc.
Jing-Qiao Lu
RayBiotech Life, Inc.
Brianne Petritis
RayBiotech Life, Inc.
Andy S. Huang
RayBiotech Life, Inc
Xin-Guang Yang
Guangzhou Medical University Second Affiliated Hospital
Youming Long (youminglong@126.com)
Guangzhou Medical University
Ruo-Pan Huang
RayBiotech, Inc.

Research

Keywords: NMOSD, AQP-4, MS, AQP-4-IgG seronegative, IL-17B, GCP-2

Posted Date: February 11th, 2021

DOI: https://doi.org/10.21203/rs.3.rs-181367/v1

Abstract

Objective

The aims of this study were to determine whether the expression levels of serological cytokines could distinguish 1) neuromyelitis optical spectrum disorders (NMOSD) from healthy controls (HCs); and 2) NMOSD patients with and without the aquaporin-4 (AQP-4) antibody biomarker from each other; and 3) NMOSD patients without antibody to AQP-4 from multiple sclerosis (MS).

Methods

The expression levels of 200 proteins in serum from 41 NMOSD (32 with antibodies to AQP-4, 9 without antibodies to AQP-4), 12 MS patients, and 34 HCs were measured using glass-based antibody arrays. In parallel, the correlation between protein expression in NMOSD/MS patients and clinical traits was analyzed with Weighted Gene Co-expression Network Analysis (WGCNA).

Results

Thirty-nine serological proteins were differentially expressed in NMOSD patients compared to HCs. 29 differentially-expression proteins (DEPs) were specific to NMOSD whereas 10 of these were observed in NMOSD and MS samples. In addition, there were 15 DEPs between AQP-4-IgG seronegative and AQP-4-IgG seropositive NMOSD patients, and 9 DEPs between NMOSD and MS patients who did not have AQP-4-IgG.

Conclusions

Our findings highlight that serological Interleukin-17B (IL-17B) may be key biomarker of NMOSD and MS. While epidermal growth factor (EGF) may be correlated with the breakdown of the blood-brain barrier in NMOSD patients, granulocyte chemotactic protein-2 (GCP-2) and monocyte differentiation antigen CD14 (CD14) may play different roles in the pathogenesis of AQP-4-IgG seronegative and seropositive NMOSD and MS. Novel biomarkers identified in our study could potentially be used in the diagnosis and treatment of NMOSD.

Trial registration

Public title: Multi-Center Clinical Study of GFAP Astrocytopathy

Registration number: ChiCTR2000041291

Date of registration: 2020-12-23 (Retrospective registration)

URL of trail registry record: http://www.chictr.org.cn/showproj.aspx?proj=65306

Introduction

Neuromyelitis optical (NMO) is a rare and severe inflammatory demyelinating disorder of the central nervous system (CNS), which mainly affects the optic nerves and spinal cord [1]. The discovery of a specific serum biomarker, an autoantibody against aquaporin-4 (AQP-4-IgG), has helped distinguish NMO from multiple sclerosis (MS) and expand the NMO diagnosis to include neuromyelitis optical spectrum disorder (NMOSD)[2, 3]. AQP-4 is the most abundant water channel in the mammalian CNS. It is highly expressed in the membrane of astrocytic end feet at the interfaces between blood/cerebrospinal fluid and brain parenchyma [4]. Binding of AQP-4–IgG to astrocytic AQP-4 initiates neuroinflammation [5].

About 20%–40% of patients with clinical signs of NMOSD do not have AQP-4-IgG in their serum and the underlying pathogenesis in these patients is unclear [6]. In addition to AQP-4-IgG, growing evidence suggests that complements, cytokines, and chemokines also contribute to the complex pathogenesis of NMOSD [7-9]. Cytokines play an important role in innate immunity, apoptosis, angiogenesis, cell growth, and differentiation, while chemokines are associated with the recruitment of leukocytes and other inflammatory cell types. However, only limited numbers of cytokines have been tested and the results have been inconsistent [10]. Since most studies have used samples from AQP-4-IgG seropositive (AQP-4+) patients, little data have been collected from AQP-4-IgG seronegative (AQP-4-) patients.

The identification of additional NMOSD biomarkers for accurate diagnosis has been limited by disease rarity and detection techniques. While imaging techniques and cerebrospinal fluid (CSF) can provide valuable information about CNS diseases, the collection of blood samples for diagnosis is less invasive, more convenient, and economical. Therefore, in this study we aimed to screen 200 different proteins to discover candidate serological biomarkers of NMOSD using antibody arrays.

Methods

Study participants

A total of 34 healthy controls (HC), 41 NMOSD patients (32 AQP-4+ patients, 6 AQP-4- patients, 3 patients with undetectable AQP-4-IgG), and 12 MS patients who fulfilled the diagnostic criteria [11] [12] were enrolled in the study. AQP-4-IgG was detected by cell-based assays as previously described [13]. A dilution of 1:10 was the cutoff for positive and negative cases. Clinical and demographic data are summarized in **Table 1** and **Supplementary Table 1**.

Serum preparation

All serum samples were processed following standard procedures and were frozen at -80 °C until use. Written informed consent was provided by all participants. All clinical serum samples used in the study were approved by the committees for ethical review of research involving human subjects at the Second Affiliated Hospital of Guangzhou Medical University (Guangzhou, China).

Cytokines determination

The concentrations of 200 circulating cytokines in serum were measured using the Human Cytokine Array Q4000 (QAH-CAA-4000, RayBiotech, Georgia, USA), which is a high density, quantitative antibody array. A list of these proteins is provided in Supplemental Information, **Supplementary Table 2**. Serum samples were processed with the antibody arrays according to the manufacturer's protocol. Briefly, after 60 min of incubation with blocking buffer, 100 µL of 2-fold diluted serum samples were added to the array. After overnight incubation at 4 °C and extensive washing, the biotin-labeled detection antibody was added for 1 hour (h) at room temperature and then removed via washing. Alexa Fluor 555-conjugated streptavidin was then added and incubated for 1 h at room temperature. The signals were scanned and extracted using an InnoScan 300 scanner (Innopsys, Carbonne, France).

Data processing and figure generation

All the protein values were transformed with log2 transformation to facilitate data analysis, including principal component analysis (PCA), volcano plot, correlation heatmap, support vector machine (SVM) model, regularized discriminant analysis (RDA) model, and gradient boosting machine (GBM) construction. All data processing and statistical tests were performed in open source R (R Foundation for Statistical Computing, Vienna, Austria) and RStudio (RStudio, Massachusetts, USA). Figures were generated directly in RStudio and then arranged for publishing using Photoshop CS5 (Adobe, California, USA). Differentially-expressed proteins (DEPs) were defined as those with *p*-adjusted (*p*-adj) or $p < 0.05$ and absolute log2 fold change (FC) > 0.263. DEPs were represented in a volcano plot using the ggplot function in R studio.

Relationship between protein expression and clinical traits

The relationships between modules or protein expression levels in NMOSD/MS patients and clinical traits were analyzed with Weighted Gene Co-expression Network Analysis (WGCNA) with the R/Bioconductor package "WGCNA." Modules with external traits were correlated and represented as a grid with the corresponding correlation and p-value. Relationships among modules were summarized by circos plots using the "circlize" package in R and heatmap plots of the corresponding module network using the function "labeled Heatmap" in the "WGCNA" package.

Differential co-expression analysis

To assess changes in co-expression, we calculated the Spearman correlation between each protein module specific to the NMOSD or MS condition and then subtracted these correlations from healthy controls, creating co-expression and differential co-expression networks using the "WGCNA" package in R. Modules of highly correlated proteins were clustered and summarized.

Supervised diagnosis model building

Proteins that were NMOSD-specific and correlated with clinical traits helped construct a classification model. A supervised SVM model was conducted to classify NMOSD patients with healthy controls using the R package "caret." The SVM model was built using a scheme of 3-fold cross-validation with a 5-time

repeat. The model performance was evaluated using area under the curve (AUC) analysis and a confusion matrix on model prediction.

Results

Clinical presentation and cytokine detection

The demographic and clinical characteristics of 41 NMOSD patients, 12 MS patients, and 34 HC are described in **Table 1**. Magnetic resonance imaging (MRI) and optical features of NMOSD are described in **Supplementary Table 1**.

Table 1. Clinical presentation of NMOSD patients, MS patients, and HC

	HC	NMOSD	MS
Age (Mean ± SEM)	41.88 ± 2.385	41.20 ± 2.429	32.83 ± 4.071
Number	34	41	12
Sex, female:male	17:17	36:5	4:8
EDSS	n/a	2.83	1.83
AQP-4+ %	n/a	78.0 %	0 %

EDSS: expanded disability status scale

The relative levels of 200 unique proteins were measured using antibody arrays, and the resulting data were subjected to two parallel analyses: differential expression analysis and co-expression network analysis (Figure1a). The co-expression network analysis aimed to integrate both molecular and clinical data.

The statistical significance and fold change of the protein levels between NMOSD patients and HCs are displayed in a volcano plot (Figure1b). Expression levels of 39 cytokines of 200 proteins measured differed between NMOSD patients and HCs (Figure1b, red points). A PCA depicting 39 DEPs is shown in Figure1c. Hierarchical clustering of the 39 DEPs demonstrate that there are clear differences between NMOSD patients and HCs (Figure1d).

To help determine whether the DEPs are specific to NMOSD or demyelinating disease in general, we collected serum from an additional 12 patients with MS. Among the cytokines examined, the expression levels of 12 cytokines differed between MS patients and HCs (Figure2a). The PCA of all the 12 DEPs are shown in Figure 2B. Hierarchical clustering of these 12 proteins illustrate a difference between MS and HCs (Figure2c).

Functional profiling of the NMOSD-specific predictors.

Interestingly, 29 DEPs were NMOSD-specific (Figure3a, green box) and 2 proteins were MS-specific (Figure3a). After filtering multicollinear variances, the AUCs of 20 NMOSD-specific proteins were > 0.65 (Figure3b). To estimate the discrimination accuracy of the NMOSD-specific proteins, three supervised models (RDA, SVM, GBM) for 5 proteins were conducted to classify NMOSD patients from HCs. The GBM and SVM models distinguished NMOSD patients from HCs with 100% accuracy, 100% sensitivity, and 100% specificity. The RDA model classified NMOSD patients and HCs with 86.67% accuracy, 88.24% sensitivity, and 85.37% specificity (Figure3c). The protein concentrations of growth-regulated alpha protein (GRO), EGF, and TNF superfamily member 14 (LIGHT) in NMOSD patients and HCs are shown in Figure 3d.

There were 10 DEPs in both NMOSD and MS conditions compared to HCs, which include IL-17B, brain-derived neurotrophic factor (BDNF), IL-18 BPa, Angiopoietin-1 (ANG-1), Eotaxin-2, thymus and activation-regulated chemokine (TARC), GCP-2, CD40L, CD14, and Opsin-5 (OPN) (Figure 3a, blue box, inset). These proteins had an up/up or down/down trend, respectively, which indicates that a more general mechanism of the inflammatory demyelinating disease likely exists.

Differentially co-expressed modules between NMOSD and MS

Changes in protein levels provide a binary view of NMOSD (i.e., levels significantly change or not). However, disease is a gradual process as a patient's optic nerve, spinal cord, or motor disability become increasingly impaired or affected. Therefore, the differential co-expression was analyzed to identify functional modules that may be significantly associated with the measured clinical traits.

A total of 9 differentially co-expressed protein modules were identified, with each module assigned a specific color in Figure 4a. Seven (7) distinct clusters of module proteins with highly similar or different correlation profiles between NMOSD and MS conditions are indicated as "a-g" in Figure 4a. The brown and magenta modules were significantly and highly correlated with each other in patients with MS compared to patients with NMOSD. The functions of the proteins in the brown module are related to the MAPK signaling pathway. Notably, the expression levels of these proteins are significantly different in the serum of MS and NMOSD patients, thus reflecting different disease pathologies.

Next, the correlations between co-expressed protein modules and clinical traits were determined. The blue module was moderately and positively associated with Erythrocyte Sedimentation Rate (ESR) (r=0.47, p=4e-07). The blue (r=0.43, p=0.002 and r=0.4, p-0.003) and pink (r=0.41, p=0.003 and r=0.44, p=0.001) modules were moderately and positively associated with cholesterol (CHOL) and low-density lipoprotein (LDL). The turquoise module was moderately and negatively associated with total protein (TP) (r=-0.51, p=1e-04), globulin (GLB) (r=-0.4, p=0.003), and adenosine deaminase (ADA) (r=-0.46, p=7e-04).

The correlations between 30 proteins (i.e., 29 NMOSD-specific proteins and IL-6R) and clinical traits were explored. Both a circos plot and a heatmap showed protein-trait associations (Figure 4b - c). Vascular endothelial growth factor C (VEGF-C) (r=0.52, p=0.003), myeloid progenitor inhibitory factor 1 (MPIF-1) (r=0.54, p=0.002), and neuronal cell adhesion molecule (NrCAM) (r=0.53, p=0.003) were positively

associated with AQP-4-IgG titer. EGF was positively associated with ESR (r= 0.57, p=0.001). Mast/stem cell growth factor receptor kit (SCF R) and IL-6R were positively associated with serum amylase (AMS) (r= 0.58, p=8e-04 and r=0.54, p=0.002, respectively).

Serum cytokine profile analysis based on presence of AQP-4-IgG

Next, we sought to determine whether the presence of AQP-4-IgG in serum had distinct cytokine characteristics within the NMOSD cohort. When the serum proteins were analyzed based on the presence or absence of AQP-4-IgG, 15 proteins ($p < 0.05$ and absolute log2 FC > 0.263) differed between AQP-4+ and AQP-4- NMOSD patients (Figure 5a, red points). The PCA of all 15 DEPs are shown in Figure 5b. Clustering of the 15 different proteins illustrated clear differences between AQP-4+ and AQP-4- NMOSD patients (Figure 5c). Meanwhile, only 2 cytokines (IL-29, MPIF-1) differed between HCs and NMOSD patients (data not shown). Importantly, 9 cytokines ($p < 0.05$ and absolute log2 FC> 0.263) differed between AQP-4-IgG seronegative NMOSD and MS patients (Figure 5d). The PCA of the 9 DEPs are shown in Figure 5e. Hierarchical clustering of the 9 DEPs illustrate clear differences between the two groups (Figure 5f). Interestingly, the expression of GCP-2 and CD14 not only differed between AQP-4+ and AQP-4- NMOSD patients, but also differed between AQP-4- NMOSD and MS patients (Figure 5g).

Discussion

The identification of diagnostic biomarkers for NMOSD is hampered by disease rarity. Although imaging techniques and interrogation of CSF may provide more direct information on CNS disease, the collection of blood samples is less invasive, time intensive, and costly. Here, we analyzed the levels of 200 serum cytokines and chemokines, validating previously identified bio-markers and study identifying 29 new NMOSD-specific proteins compared to HCs. Moreover, we show that 10 of these DEPs are shared between NMOSD and MS patients. Fifteen cytokines were differentially expressed between AQP-4-IgG+ and AQP-4- NMOSD patients. Nine DEPs between AQP-4- NMOSD and AQP-4- MS patients were also identified.

The breakdown of the blood–brain barrier (BBB) is a key pathogenic step in the initiation and progression of NMOSD. As the BBB breaks down, AQP-4-IgG synthesized in the peripheral lymphoid cells can cross the BBB to bind to astrocytic AQP4 receptors, which leads to complement dependent cytotoxicity (CDC) and antibody-dependent cell-mediated cytotoxicity (ADCC). Although infusion of serum with positive AQP4 antibody to experimental autoimmune encephalomyelitis (EAE) rats with broken blood-brain barrier caused NMO-like lesions, when it was infused into healthy rats, no NMO lesions were seen[14]. Autoantibodies against human brain microvascular endothelial cells (BMECs) other than anti-AQP4 antibodies may disrupt the BBB through upregulation of VEGF in BMECs[15]. There may be other serological components correlated with BBB disruption in NMOSD.

The interleukin (IL)-17 superfamily, a relatively new family of cytokines, consists of six ligands (IL-17A to IL-17F). IL-17A is one of the T helper (Th) 17 cells and Th17-associated interleukins that are the key effectors of autoimmune inflammatory demyelination diseases, including MS and NMOSD[16]. A previous study indicated that IL-17A augments reactive oxygen species production that leads to the

breakdown of the BBB [17]. Unlike IL-17A and IL-17F, which are mainly produced by Th17 cells, IL-17B is widely expressed in various tissues and cell types [18, 19]. Interestingly, IL-17B is highly abundant in neutrophils. Several experimental findings strongly support the role of IL-17B in the pathogenesis of inflammatory arthritis and systemic lupus erythematosus because IL-17B is significantly elevated in these patients compared to healthy controls[20]. However, studies of IL-17B/IL-17RB signaling on demyelination diseases are scant, especially for NMOSD. In our study, we found that IL-17B and CXCL1 were significantly increased in the serum of NMOSD patients compared with healthy controls, suggesting that IL-17B may be involved in the pathogenesis progression of NMOSD. Importantly, IL-17B mRNA is expressed at very high levels in the spinal cord and IL-17B protein primarily localizes to neuronal cell bodies and axons[21, 22]. Further research is needed to obtain a complete understanding of the biological function of IL-17B in NMOSD.

The EGF signaling pathway plays important roles in proliferation, differentiation, and migration of a variety of cell types, especially in epithelial cells. Previous studies have reported that the secretion of EGF in peripheral blood mononuclear cells (PBMCs) of patients with relapsing remitting multiple sclerosis (RR-MS) is highly dysregulated compared with HCs[23]. However, other studies demonstrated that the expression levels of EGF and its receptor (EGFR) are reduced in MS spinal cord and lesions[24]. Treatment with anti-EGF antibodies ameliorate EAE via induction of neurogenesis and oligodendrogenesis[25]. Exogenous EGF treatment reduces demyelination lesions in an EAE mouse model and results in neuroprotection in both neonatal and adult mouse models of brain injury by stimulating proliferation and maturation of oligodendrocyte precursor cells (OPCs)[26, 27]. Moreover, EGF protein expression could improve BBB integrity against ischemic injury by upregulating the expression of tight junction proteins[28].

Though the role of EGF in the pathogenesis of MS has been explored in previous studies, little is known about its function in NMOSD. Our results show that serological EGF levels in NMOSD patients were significantly higher than in HCs. Whether the increased level of EGF in NMOSD patients' serum can alter the expression of TJ proteins and contribute to the breakdown of BBB remain unknown. In addition, women are preferentially affected with NMOSD with a female:male ratio of nearly 10:1. There is a sexual dimorphism of EGF concentrations in both kidney and urine, with higher EGF levels in females[29]. Whether the increased serum EGF in NMOSD is associated with the pathogenesis of NMOSD needs to be further examined.

Misdiagnosing NMOSD as MS occurs frequently (40%) [30], even though the diseases have different prognoses and treatments. For example, the prognosis for NMOSD patients is usually worse and some MS therapies, such as interferon-b, natalizumab, or fingolimod, may be ineffective or harmful to NMOSD patients [31]. Moreover, experts frequently disagree on the diagnosis and treatment of AQP-4-IgG negative NMOSD and MS patients. Our data indicate that GCP-2 may be influencing the immunopathogenesis of AQP-4+ and AQP-4- NMOSD patients as well as MS patients.

GCP-2/CXCL6 is an important member of the ELR + CXC chemokine family and assists in recruiting cells, such as neutrophils, hyaline leukocytes, macrophages, and lymphocytes to sites of inflammation. In this study, the serological levels of GCP-2 correlated with the AQP-4-IgG titer in NMOSD patients but not in MS patients. More specifically, the GCP-2 expression was decreased in AQP-4-IgG seronegative NMOSD patients but increased in AQP-4-IgG seropositive NMOSD and MS patients. We observed the same trend in this study. For the first time, we demonstrate that the serum level of 9 proteins differed between AQP-4-IgG seronegative NMOSD and MS patients (Figure 5F). These data could help to diagnose patients properly since distinguishing AQP-4 Ab-seronegative NMOSD and optical spinal predominant MS from each other remains a clinical challenge. Finally, a previous study showed that GCP-2 levels were significantly higher in AQP-4-IgG seropositive patients compared to the myelin oligodendrocyte glycoprotein antibody (MOG-IgG) seropositive group [32].

Further studies using larger independent cohorts are needed to assess proteomic differences between acute and relapsed NMOSD patients, and to determine the correlations between disease severity and treatment response. Such data will help to validate our results and develop diagnostic algorithms for NMOSD. This is especially true for the heterogeneous group of AQP-4-IgG seronegative NMOSD patients. It is important to note that prior immunosuppressive or immunomodulatory treatment taken by the patients in our study may have influenced the results.

Conclusion

Our study identified that IL-17B may be key cytokine marker of NMOSD and MS patients in serum, while EGF may be correlated with the breakdown of the BBB in NMOSD patients. GCP-2 and CD14 may help distinguish the immunopathogenesis of AQP-4-IgG seronegative and seropositive NMOSD as well as MS. Serological levels of GCP-2 of AQP-4-IgG seronegative NMOSD patients differed from AQP-4-IgG seropositive NMOSD and MS patients, which may be an influencing factor in demyelination disease. Our findings shed further light on the potential roles of specific inflammatory mediators and growth factors in the immunopathogenesis. These proteins may aid in diagnosing and treating demyelinating disorders.

Abbreviations

NMO: neuromyelitis optical; CNS: central nervous system; AQP-4: aquaporin-4; MS: multiple sclerosis; NMOSD: neuromyelitis optical spectrum disorder; CSF: cerebrospinal fluid; SVM: support vector machine; RDA: regularized discriminant analysis; GBM: gradient boosting machine; DEPs: differentially-expressed proteins; WGCNA: Weighted Gene Co-expression Network Analysis; AUC: area under the curve; MRI: magnetic resonance imaging; EDSS: expanded disability status scale; ESR: Erythrocyte Sedimentation Rate; CHOL: cholesterol; LDL: low-density lipoprotein; TP: total protein; GLB: globulin; ADA: adenosine deaminase; BBB: blood–brain barrier; CDC: complement dependent cytotoxicity; ADCC: antibody-dependent cell-mediated cytotoxicity; EAE: experimental autoimmune encephalomyelitis; BMECs: brain microvascular endothelial cells; RR-MS: relapsing remitting multiple sclerosis; OPCs: oligodendrocyte precursor cells; MOG-IgG: myelin oligodendrocyte glycoprotein antibody; IL-17B: Interleukin-17B; CD14:

Monocyte differentiation antigen CD14; EGF: epidermal growth factor; GCP-2: granulocyte chemotactic protein-2; GRO: growth-regulated alpha protein; LIGHT: TNF superfamily member 14 ; BDNF: brain-derived neurotrophic factor; ANG-1: Angiopoietin-1; TARC: thymus and activation-regulated chemokine ; OPN: Opsin-5; VEGF-C: vascular endothelial growth factor C;

MPIF-1: myeloid progenitor inhibitory factor 1; NrCAM: neuronal cell adhesion molecule; SCF R: mast/stem cell growth factor receptor kit.

Declarations

Ethics approval and consent to participate:

The study protocol (NO.2019-hs-11,2020-hs-54) was approved by the Ethics Committee of the Second Affiliated Hospital of Guangzhou Medical University, China. All the patients in the present study provided informed consent.

Consent for publication:

All the patients in the present study provided informed consent.

Availability of data and material:

Anonymized data will be shared upon request from qualified investigators.

Competing interests:

C. Gao, X.G. Yang and Y.M. Long report no disclosures.

C.C. Fu, H.H. Zhang, Y.Q. Mao, J.Q. Lu, B. Petritis, A. S. Huang and R.P. Huang are employees of RayBiotech, Inc., which developed the antibody arrays used in this study.

Funding:

This study was supported by the National Natural Science Foundation of China (81771302), Science and Technology Program of Guangzhou, China (201803010123), the RayBiotech Innovative Research Fund, Guangzhou Innovation Leadership Team (CXLJTD-201602), Pearl River S&T Nova Program of Guangzhou

(201806010035, 201806010032), Guangdong Province Key Technologies R&D Program for "Precision Medicine and Stem Cells" (2019B020227004), National Science and Technology Major Project of China (No.2018ZX10732-401-003-012), the Industry-University-Research Collaborative Innovation Special Project of Guangzhou

(201802030001), Guangzhou Basic and Applied Basic Research Project (202002030242) and the General Project of Guangzhou Science and Technology Research Program (201707010438; 201707010392).

Guangzhou Science and Technology Program key projects (202002020021).

Authors' contributions:

C.C. Fu: Drafting/revision of the manuscript for content, including medical writing for content; Study concept or design; Analysis or interpretation of data. C. Gao: Study concept or design. H.H. Zhang: Analysis or interpretation of data. Y.Q. Mao and A.S. Huang: Analysis or interpretation of data; Additional contributions: Array design and preparation. J.Q. Lu: Analysis or interpretation of data. B. Petritis: Drafting/revision of the manuscript for content, including medical writing for content. X.G. Yang: Study concept or design. Y.M. Long: Major role in the acquisition of data; Study concept or design. R.P. Huang: Initiating and directing entire project; Drafting/revision of the manuscript for content; Major role in the acquisition of data; Study concept or design; Analysis or interpretation of data.

Acknowledgements:

Not applicable

References

1. Jarius S, Paul F, Franciotta D, Waters P, Zipp F, Hohlfeld R, Vincent A, Wildemann B: Mechanisms of disease: aquaporin-4 antibodies in neuromyelitis optica.*Nat Clin Pract Neurol* 2008, 4:202-214.
2. Lennon VA, Wingerchuk DM, Kryzer TJ, Pittock SJ, Lucchinetti CF, Fujihara K, Nakashima I, Weinshenker BG: A serum autoantibody marker of neuromyelitis optica: distinction from multiple sclerosis.*The Lancet* 2004, 364:2106-2112.
3. Jarius S, Franciotta D, Bergamaschi R, Wright H, Littleton E, Palace J, Hohlfeld R, Vincent A: NMO-IgG in the diagnosis of neuromyelitis optica.*Neurology* 2007, 68:1076-1077.
4. Lennon VA, Kryzer TJ, Pittock SJ, Verkman AS, Hinson SR: IgG marker of optic-spinal multiple sclerosis binds to the aquaporin-4 water channel.*J Exp Med* 2005, 202:473-477.
5. Takahashi T, Fujihara K, Nakashima I, Misu T, Miyazawa I, Nakamura M, Watanabe S, Shiga Y, Kanaoka C, Fujimori J, et al: Anti-aquaporin-4 antibody is involved in the pathogenesis of NMO: a study on antibody titre.*Brain* 2007, 130:1235-1243.
6. Kitley J, Leite MI, Kuker W, Quaghebeur G, George J, Waters P, Woodhall M, Vincent A, Palace J: Longitudinally extensive transverse myelitis with and without aquaporin 4 antibodies.*JAMA Neurol* 2013, 70:1375-1381.
7. Lucchinetti CF, Mandler RN, McGavern D, Bruck W, Gleich G, Ransohoff RM, Trebst C, Weinshenker B, Wingerchuk D, Parisi JE, Lassmann H: A role for humoral mechanisms in the pathogenesis of Devic's neuromyelitis optica.*Brain* 2002, 125:1450-1461.
8. Uzawa A, Mori M, Arai K, Sato Y, Hayakawa S, Masuda S, Taniguchi J, Kuwabara S: Cytokine and chemokine profiles in neuromyelitis optica: significance of interleukin-6.*Mult Scler* 2010, 16:1443-1452.

9. Uzawa A, Mori M, Kuwabara S: Cytokines and chemokines in neuromyelitis optica: pathogenetic and therapeutic implications.*Brain Pathol* 2014, 24:67-73.
10. Michael BD, Elsone L, Griffiths MJ, Faragher B, Borrow R, Solomon T, Jacob A: Post-acute serum eosinophil and neutrophil-associated cytokine/chemokine profile can distinguish between patients with neuromyelitis optica and multiple sclerosis; and identifies potential pathophysiological mechanisms - a pilot study.*Cytokine* 2013, 64:90-96.
11. Wingerchuk DM, Banwell B, Bennett JL, Cabre P, Carroll W, Chitnis T, de Seze J, Fujihara K, Greenberg B, Jacob A, et al: International consensus diagnostic criteria for neuromyelitis optica spectrum disorders.*Neurology* 2015, 85:177-189.
12. Thompson AJ, Banwell BL, Barkhof F, Carroll WM, Coetzee T, Comi G, Correale J, Fazekas F, Filippi M, Freedman MS, et al: Diagnosis of multiple sclerosis: 2017 revisions of the McDonald criteria.*Lancet Neurol* 2018, 17:162-173.
13. Long Y, Liang J, Zhong R, Wu L, Qiu W, Lin S, Gao C, Chen X, Zheng X, Yang N, et al: Aquaporin-4 antibody in neuromyelitis optica: re-testing study in a large population from China.*Int J Neurosci* 2017, 127:790-799.
14. Bradl M, Misu T, Takahashi T, Watanabe M, Mader S, Reindl M, Adzemovic M, Bauer J, Berger T, Fujihara K, et al: Neuromyelitis optica: pathogenicity of patient immunoglobulin in vivo.*Ann Neurol* 2009, 66:630-643.
15. Shimizu F, Sano Y, Takahashi T, Haruki H, Saito K, Koga M, Kanda T: Sera from neuromyelitis optica patients disrupt the blood-brain barrier.*J Neurol Neurosurg Psychiatry* 2012, 83:288-297.
16. Agasing AM, Wu Q, Khatri B, Borisow N, Ruprecht K, Brandt AU, Gawde S, Kumar G, Quinn JL, Ko RM, et al: Transcriptomics and proteomics reveal a cooperation between interferon and T-helper 17 cells in neuromyelitis optica.*Nat Commun* 2020, 11:2856.
17. Huppert J, Closhen D, Croxford A, White R, Kulig P, Pietrowski E, Bechmann I, Becher B, Luhmann HJ, Waisman A, Kuhlmann CR: Cellular mechanisms of IL-17-induced blood-brain barrier disruption.*FASEB J* 2010, 24:1023-1034.
18. Bie Q, Jin C, Zhang B, Dong H: IL-17B: A new area of study in the IL-17 family.*Mol Immunol* 2017, 90:50-56.
19. Kouri VP, Olkkonen J, Ainola M, Li TF, Bjorkman L, Konttinen YT, Mandelin J: Neutrophils produce interleukin-17B in rheumatoid synovial tissue.*Rheumatology (Oxford)* 2014, 53:39-47.
20. Robak E, Kulczycka-Siennicka L, Gerlicz Z, Kierstan M, Korycka-Wolowiec A, Sysa-Jedrzejowska A: Correlations between concentrations of interleukin (IL)-17A, IL-17B and IL-17F, and endothelial cells and proangiogenic cytokines in systemic lupus erythematosus patients.*Eur Cytokine Netw* 2013, 24:60-68.
21. Shi Y, Ullrich SJ, Zhang J, Connolly K, Grzegorzewski KJ, Barber MC, Wang W, Wathen K, Hodge V, Fisher CL, et al: A novel cytokine receptor-ligand pair. Identification, molecular characterization, and in vivo immunomodulatory activity.*J Biol Chem* 2000, 275:19167-19176.

22. Moore EE, Presnell S, Garrigues U, Guilbot A, LeGuern E, Smith D, Yao L, Whitmore TE, Gilbert T, Palmer TD, et al: Expression of IL-17B in neurons and evaluation of its possible role in the chromosome 5q-linked form of Charcot-Marie-Tooth disease.*Neuromuscul Disord* 2002, 12:141-150.
23. Levy YA, Fainberg KM, Amidror T, Regev K, Auriel E, Karni A: High and dysregulated secretion of epidermal growth factor from immune cells of patients with relapsing-remitting multiple sclerosis.*J Neuroimmunol* 2013, 257:82-89.
24. Scalabrino G, Veber D, De Giuseppe R, Roncaroli F: Low levels of cobalamin, epidermal growth factor, and normal prions in multiple sclerosis spinal cord.*Neuroscience* 2015, 298:293-301.
25. Amir-Levy Y, Mausner-Fainberg K, Karni A: Treatment with Anti-EGF Ab Ameliorates Experimental Autoimmune Encephalomyelitis via Induction of Neurogenesis and Oligodendrogenesis.*Mult Scler Int* 2014, 2014:926134.
26. Vinukonda G, Hu F, Mehdizadeh R, Dohare P, Kidwai A, Juneja A, Naran V, Kierstead M, Chawla R, Kayton R, Ballabh P: Epidermal growth factor preserves myelin and promotes astrogliosis after intraventricular hemorrhage.*Glia* 2016, 64:1987-2004.
27. Scafidi J, Hammond TR, Scafidi S, Ritter J, Jablonska B, Roncal M, Szigeti-Buck K, Coman D, Huang Y, McCarter RJ, Jr., et al: Intranasal epidermal growth factor treatment rescues neonatal brain injury.*Nature* 2014, 506:230-234.
28. Yang S, Jin H, Zhao ZG: Epidermal growth factor treatment has protective effects on the integrity of the blood-brain barrier against cerebral ischemia injury in bEnd3 cells.*Exp Ther Med* 2019, 17:2397-2402.
29. Mattila AL: Human urinary epidermal growth factor: effects of age, sex and female endocrine status.*Life Sci* 1986, 39:1879-1884.
30. Jarius S, Ruprecht K, Wildemann B, Kuempfel T, Ringelstein M, Geis C, Kleiter I, Kleinschnitz C, Berthele A, Brettschneider J, et al: Contrasting disease patterns in seropositive and seronegative neuromyelitis optica: A multicentre study of 175 patients.*J Neuroinflammation* 2012, 9:14.
31. Trebst C, Jarius S, Berthele A, Paul F, Schippling S, Wildemann B, Borisow N, Kleiter I, Aktas O, Kumpfel T, Neuromyelitis Optica Study G: Update on the diagnosis and treatment of neuromyelitis optica: recommendations of the Neuromyelitis Optica Study Group (NEMOS).*J Neurol* 2014, 261:1-16.
32. Ai N, Liu H, Zhou H, Lin D, Wang J, Yang M, Song H, Sun M, Xu Q, Wei S: Cytokines and chemokines expression in serum of patients with neuromyelitis optica.*Neuropsychiatr Dis Treat* 2019, 15:303-310.

Figures

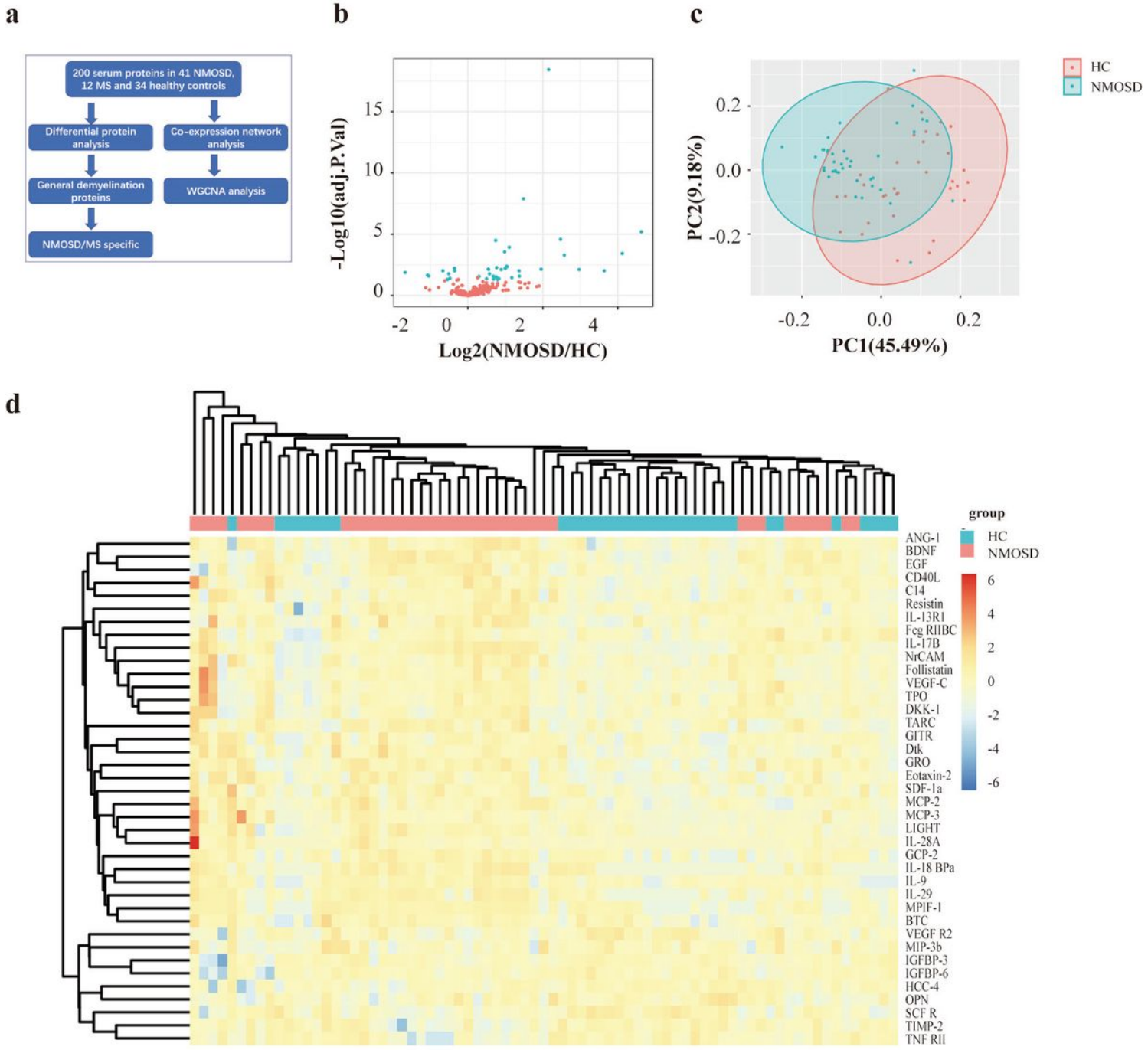

Figure 1

Antibody array analysis reveals differentially-expressed protein profiles of NMOSD patients compared with healthy controls. a. Overview of experimental and analysis workflow. The serological concentrations of 200 proteins were determined with an antibody microarray. Protein expression and co-expression network analyses for each group (NMOSD, MS, HC) were performed. b. Volcano plot showing the distribution of 200 protein expression levels between NMOSD patients and HCs (p-adj < 0.05 and absolute log2 FC > 0.263). adj.P.val = adjusted p-value. c. PCA analysis of the 39 DEPs. The first two primary components (PC1, PC2) are plotted. d. Clustering heatmap of the 39 DEPs between NMOSD patients (pink) and HCs (cyan).

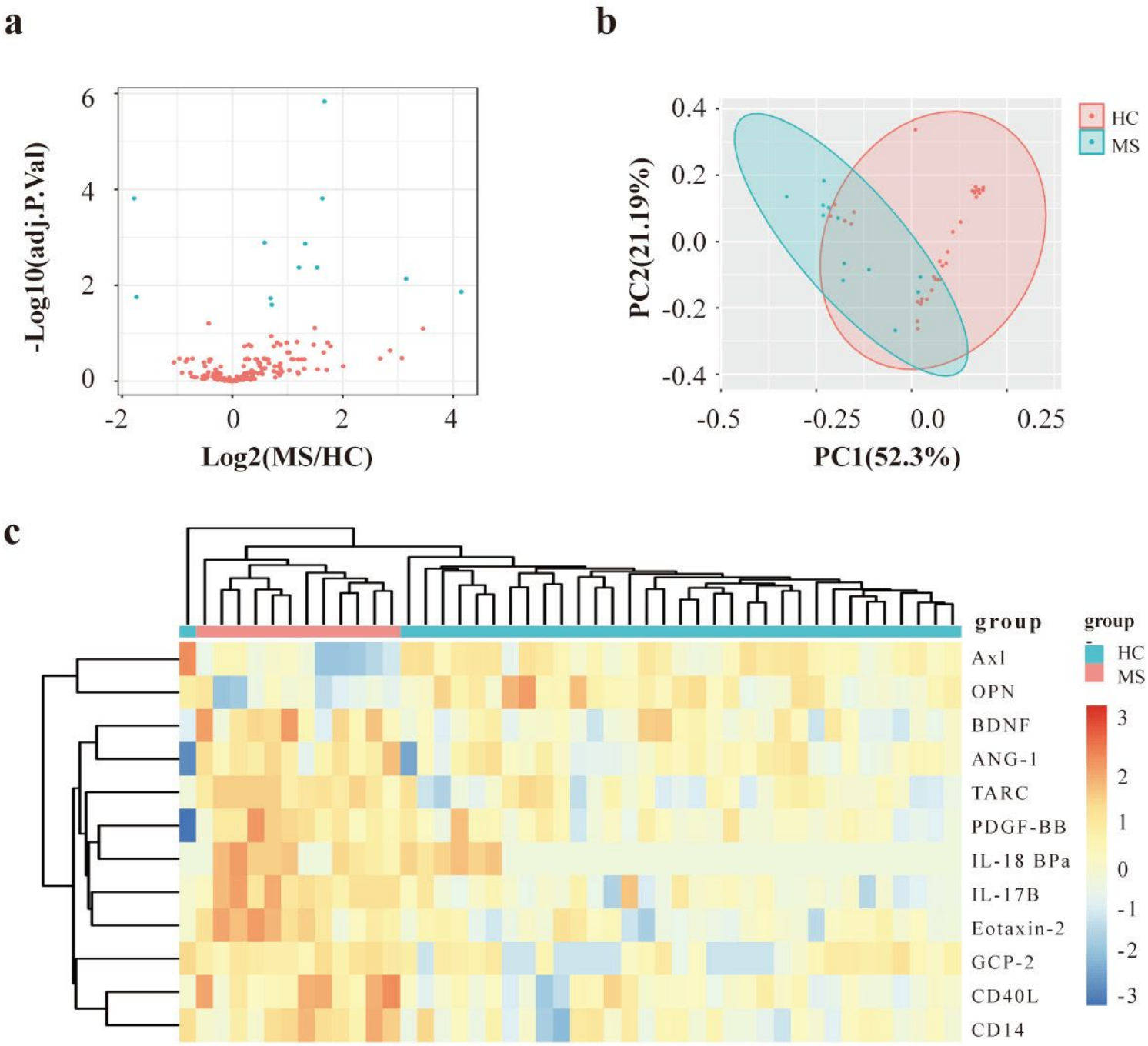

Figure 2

Antibody array reveals differentially-expressed protein profiles of MS patients compared with healthy controls. a. Volcano plot showing the distribution of 200 protein expression levels between MS patients and HCs (p-adj < 0.05 and absolute log2 FC > 0.263). adj.P.val = adjusted p-value. b. PCA analysis conducted on the 12 DEPs. The first two primary components (PC1, PC2) are plotted. c. Clustering heatmap of the 12 DEPs between MS patients (pink)and HCs (cyan).

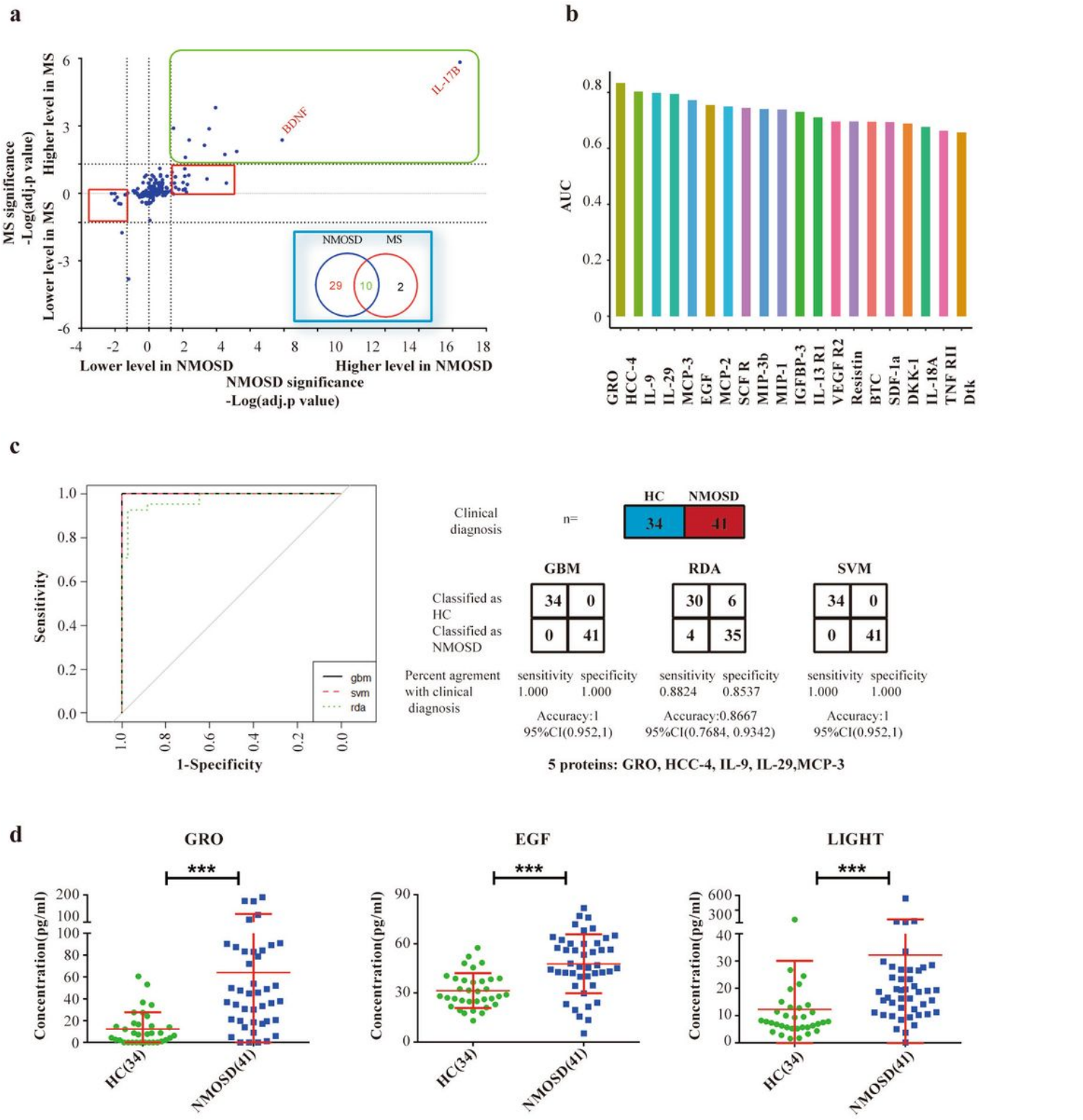

Figure 3

The plasma proteome contains disease-specific information. To assess the specificity of the proteins identified in the expression level analysis, NMOSD samples were compared to MS samples. a. Plot of the log10-transformed adjusted p-value (p-adj) of NMOSD and MS data show preserved directionality, resulting in the classification of four distinct groups: “General demyelination” (p-adj.NMOSD < 0.05 and p-adj.MS < 0.05, same direction of changes in both diseases, green box); “NMOSD specific” (p-adj.NMOSD

< 0.05, p-adj.MS>0.05; red box); “MS specific” (p-adj.MS < 0.05, p-adj.NMOSD > 0.05); “Non-significant” (p-adj.NMOSD and p-adj.MS > 0.05). A Venn diagram showing the overlap of DEPs in NMOSD and MS (inset, blue box). b. Histogram showing the AUCs of 20 NMOSD-specific proteins after filtering multicollinear variances. c. Establishment of SVM, RDA and GBM classification models for NMOSD using 5 DEPs. Left panel: receiver operating characteristic (ROC) curve of the training set using the three models. Right panel: confusion matrix used to calculate the percentage of classifications that agreed with the clinical diagnoses. d. Jitter plots of serum levels (pg/ml) of indicated proteins in the respective study groups. Each dot represents an individual sample, and the horizontal lines represent group means. *** p < 0.001.

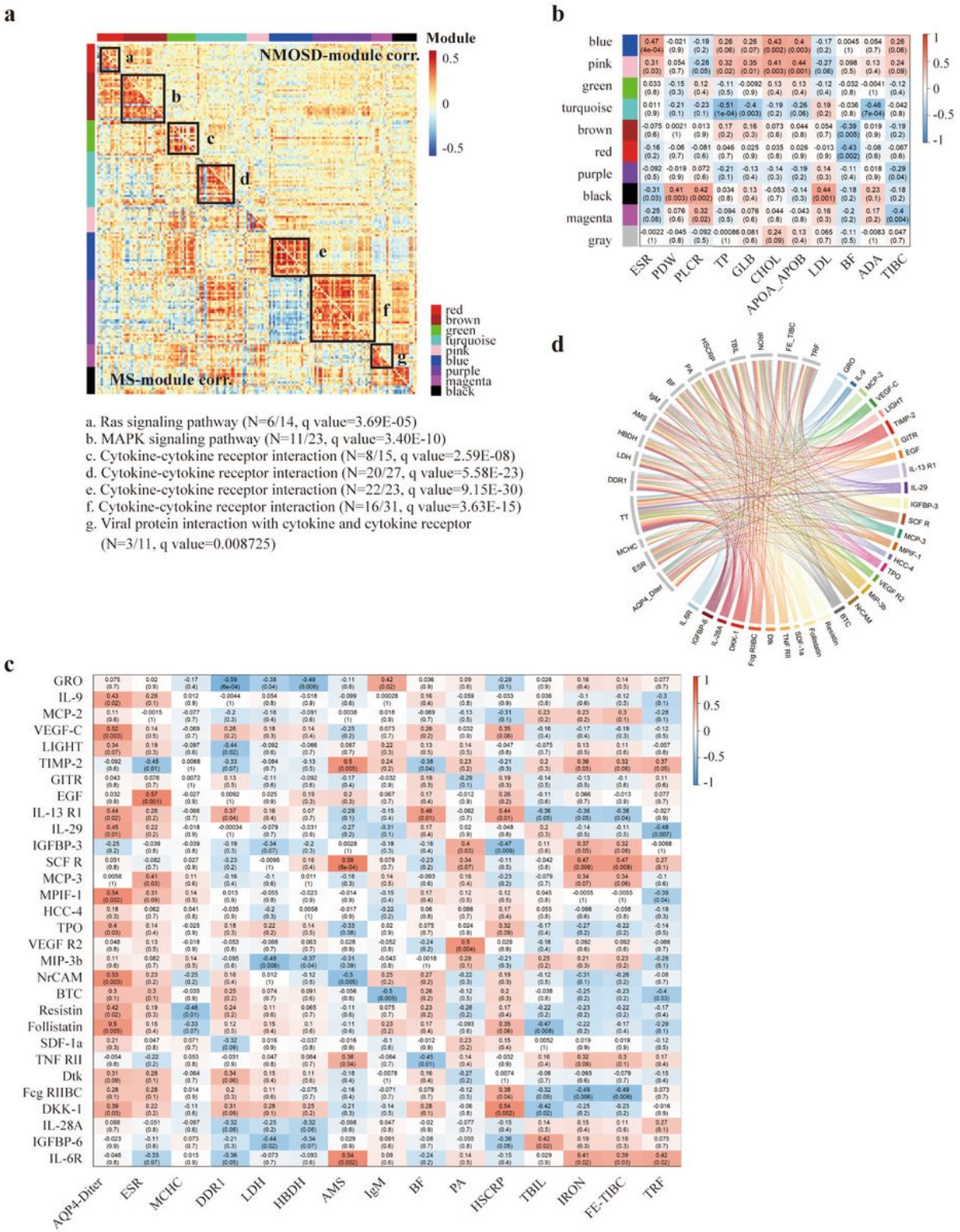

Figure 4

Differentially co-expressed modules between NMOSD and MS. a. Comparative correlation heatmap. The upper diagonal of the main matrix shows correlations between pairs of proteins among the NMOSD samples (red color = positive correlations, blue = negative correlations). The lower diagonal of the heatmap shows correlations between the same protein pairs in the MS samples. Modules are identified on the right side of the heatmap by a color bar. b. Protein module-trait associations. Each row

corresponds to a module (color) and each column to a clinical trait. 200 proteins were divided into 9 modules. Each cell contains the correlation index and p-value. Level of correlation is color-coded according to the color legend. Red = positive correlation, blue = negative correlation. c. Protein-trait associations. Each row corresponds to a protein and each column to a clinical trait. Each cell contains the correlation index and p-value. Level of correlation is color-coded according to the color legend. Red = positive correlation, blue = negative correlation. d. Circos plot showing protein-trait associations. Left side of circos plot represents traits and right side represents 30 specific proteins.

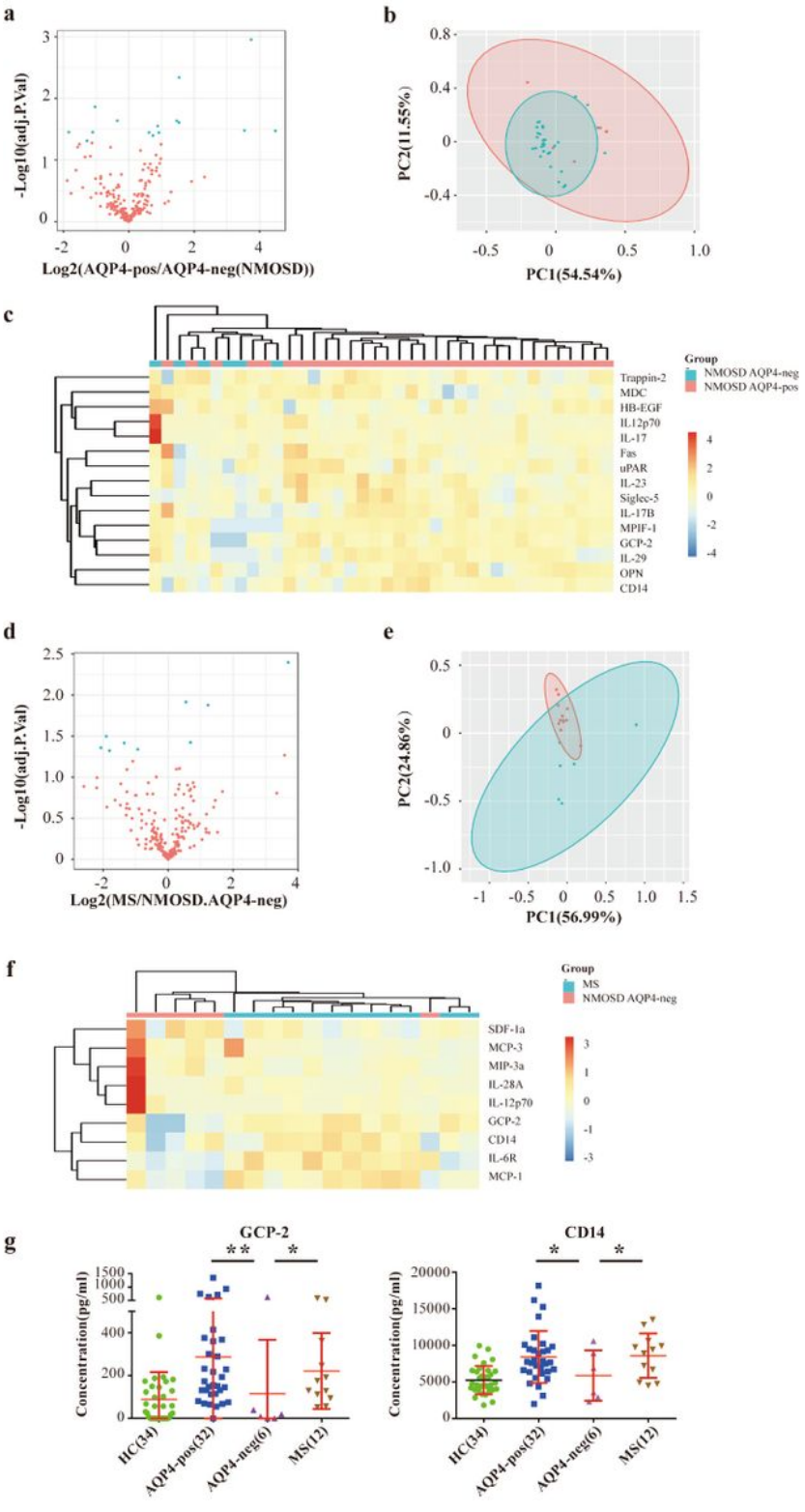

Figure 5

Serum cytokine profile analysis based on presence of AQP-4 autoantibody. a. Volcano plot showing the distribution of 200 proteins between AQP4-seronegative NMOSD patients and AQP4-seropositive NMOSD patients ($p < 0.05$ and absolute log2 FC > 0.263). b. PCA analysis conducted on the 15 DEPs. The first two primary components (PC1, PC2) are plotted. c. Clustering heatmap of the 15 DEPs between AQP4-seronegative (cyan) and AQP4-seropositive (pink) NMOSD patients. d. Volcano plot showing the distribution of 200 proteins between AQP4-seronegative NMOSD and MS patients ($p < 0.05$ and absolute log2 FC > 0.263). e. PCA analysis conducted on the 9 DEPs. The first two primary components (PC1, PC2) are plotted. f. Clustering heatmap of the 9 DEPs between AQP4-seronegative NMOSD patients (pink) and MS patients (cyan). g. Plots of serum levels (pg/ml) of indicated molecules in the respective study groups. Each dot represents an individual sample, and the horizontal lines represent group means. * $p<0.05$, ** $p<0.01$ and *** $p<0.001$.

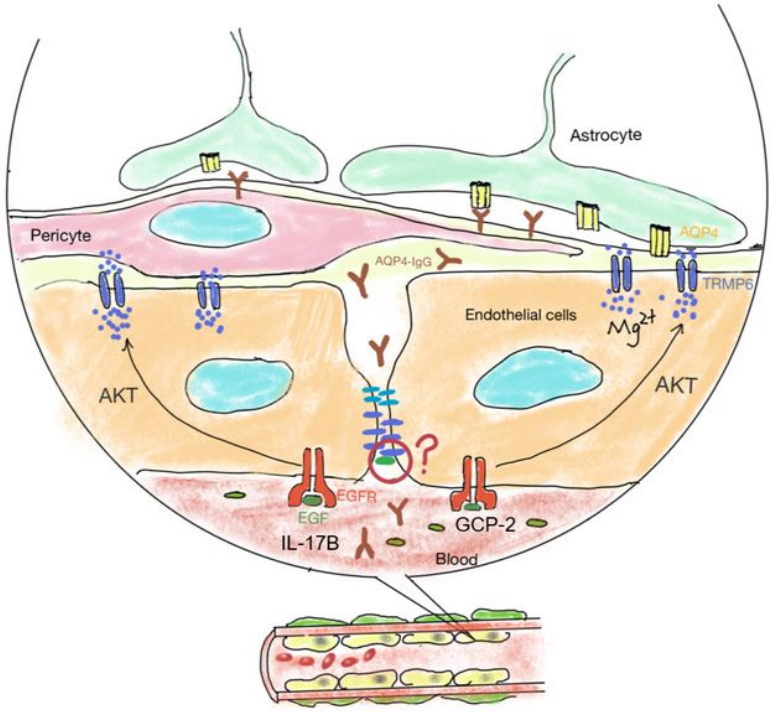

Figure 6

Hypothesis of the underlying mechanisms of NMOSD. Serological APQ4-IgG crosses the disrupted BBB and targets AQP4 channels on the end feet of astrocytes, followed by complement activation and inflammatory activation. Inflammatory recruitment and activation lead to microglia activation and oligodendrocyte loss and demyelination; these responses may correlate with increased serological levels of IL-17B, GCP-2, and CD14.

Supplementary Files

This is a list of supplementary files associated with this preprint. Click to download.

- SupplementalInformation.docx